Paper 112

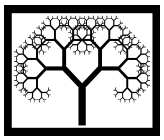

Proceedings of the Twelfth International Conference
on Computational Structures Technology,
B.H.V. Topping and P. Iványi, (Editors),
Civil-Comp Press, Stirlingshire, Scotland.

Modelling the Structural Behaviour of Rammed Earth Components

R.A. Silva[1], D.V. Oliveira[1], L. Schueremans[2], P.B. Lourenço[1] and T. Miranda[1]
[1]ISISE, Department of Civil Engineering
University of Minho, Guimarães, Portugal
[2]Department of Civil Engineering, KU Leuven, Frisomat, Belgium

Abstract

The rammed earth technique has a significant presence in the earthen built heritage, where was used to build from simple dwellings to fortresses. However, the high vulnerability of rammed earth construction to decay agents and to seismic events puts at risk their further existence and the lives of millions of people. With respect to the seismic behaviour of rammed earth walls, the understanding and modelling of their shear behaviour are topics rarely approached in literature. Nevertheless, these topics are of significant importance in the preservation and strengthening of rammed earth constructions.

This paper presents experimental and numerical work where the shear behaviour of unstabilised rammed earth is analysed. The experimental program consisted in the testing of several unstabilised rammed earth wallets subject to diagonal compression, which allowed a better understanding of the shear behaviour of unstabilised rammed earth. The numerical work consists of the modelling, of the previous tests, using the finite element method and by considering both the macro- and micro-modelling approaches. In general, the numerical models showed a good agreement with the experimental results.

Keywords: rammed earth, modelling, shear behaviour.

1 Introduction

Since ancient times that raw earth has been used for building dwellings, storehouses, windmills, temples, etc. The worldwide and large availability of this material explains its intensive use around the world, which resulted in a large and diverse earthen built stock. The large diversity of the earthen built heritage results from the fact that this type of construction is related to the concept of vernacular architecture. Several building techniques have been developed, although the most common and widespread ones are the adobe masonry and the rammed earth [1].

Building in rammed earth, also known as “taipa”, “taipa de pilão”, “tapial”, “pise de terre”, “pisé” or “stampflehm”, consists in compacting moist earth by layers inside a formwork to build monolithic walls (see Figure 1). In general, the earth used is characterized by a broad particle size distribution, ranging from clay to gravel size, which promotes a material with high density upon compaction. The addition of lime is a practice commonly observed in existing rammed earth constructions, especially in the case of military fortresses from the Iberian Peninsula [2-3], which are several hundred years old. The compaction of traditional rammed earth is carried out resorting to manual rammers made from timber, which results in a characteristic horizontal layering. In fact, the use of the formwork constitutes a key feature and differentiates this technique from other earth construction techniques [1, 4]. A traditional formwork is, in general, supported directly on the wall by means of putlogs crossing the entire thickness of the wall, and is dislocated horizontally as the rammed earth blocks are built. This means that construction of a wall is carried out by courses (like masonry), where the formwork runs horizontally along the perimeter of the construction and then is lifted to build the next course [5]. The presence of putlog holes between courses is also common and results from the removal or deterioration of the putlogs. The dimensions of the rammed earth blocks are very variable from region to region, for example in Alentejo (Portugal) the length of rammed earth blocks from typical dwellings may range from 1.40 m to 2.50 m, the height from 0.4 m to 0.55 m and the thickness from 0.4 m to 0.57 m [6].

Figure 1: New rammed earth construction in Odemira (Portugal).

The preservation of the rammed earth built heritage demands frequent conservation interventions, since this type of constructions is very sensitive to some external agents, such as rainfall, wind, rising damp, soil settlements and earthquakes. The absence of these interventions leads to the fast decay of these constructions [7] in the form of cracking, reduction of the bearing cross sections and reduction of the mechanical properties of the earthen materials. These types of damage have obvious negative impact on the structural performance of these constructions. Furthermore, earth constructions are acknowledged by an intrinsic relatively poor seismic behaviour [8], meaning that these issues are particularly sensitive in regions with non-negligible seismic hazard.

The conservation of rammed earth constructions requires deep knowledge on the material properties and failure mechanisms [9]. However, this information is still very limited and scattered in literature [10]. The numerical modelling of rammed earth is also an important tool for decision making in the conservation of this type of constructions. However, references on the modelling of rammed earth constructions are hardly found in literature. The few known studies [11-13] adopted very simple models, which included very simple constitutive laws for the materials (such as linear elastic isotropic and elastic-perfectly plastic behaviour). In general, these models were used to predict stress levels and to simulate possible collapse mechanisms. The simulation of the deformability and shear behaviour of rammed earth constructions are topics usually not addressed. However, these are fundamental for understanding and predicting the behaviour of rammed earth construction in the case of a seismic event, where their structural behaviour is expected to be governed by the highly non-linear behaviour of the material.

On the other hand, complex constitutive laws require detailed information on the properties of rammed earth materials, which is not always available or is available from a limited quantity of experimental tests. Moreover, the variability found in raw earthen materials brings up even more uncertainties regarding the characterization of the materials and to the modelling. A compromise should then be found between representativeness, reliability, accuracy and complexity of the constitutive model with respect to the material behaviour, namely regarding the computational demand of the analysis.

With respect to the seismic behaviour of rammed earth walls, both out-of-plane and in-plane behaviour should be taken into account. Nevertheless, this paper deals only with the in-plane shear behaviour. The paper initially presents an experimental program where the shear behaviour of unstabilised rammed earth (URE) representative from Alentejo (southern Portugal) is assessed. The experimental program consisted mainly in a set of diagonal compression tests on URE wallets. Then, the experimental data was used in the calibration of finite element method (FEM) models, which aimed at modelling the diagonal compression tests carried out. Both macro- and micro-modelling approaches were considered for this purpose, where the micro-modelling approach was intended to evaluate the influence of apparent weakness of the layer interfaces [14].

2 Experimental program

2.1 Methodology

In order to manufacture representative URE specimens from Alentejo, a soil from this region was collected. The properties of the soil were assessed in order to check its suitability for URE construction according to international recommendations. Correction of the particle size distribution (PSD) of the soil was observed to be required and is detailed later. With respect to the mechanical behaviour of the URE manufactured with the corrected soil, both compression and shear behaviour were characterized by means of compression and diagonal compression tests, respectively.

2.2 Soil suitability and URE specimens manufacturing

The soil was characterized by means of expeditious (sedimentation test, ribbon test, drop test and dry strength test) and laboratory tests (PSD analysis, consistency limits and standard Proctor) to assess its suitability for URE (see [15] for further details).
In general, the expeditious tests revealed that the clay content of the soil was excessively high. This observation is confirmed by the PSD curve presented in Figure 2, which shows a clay content of about 28%. Furthermore, the PSD curve of the soil does not respect the recommended PSD envelope for rammed earth suggested by Houben and Guillaud [1].

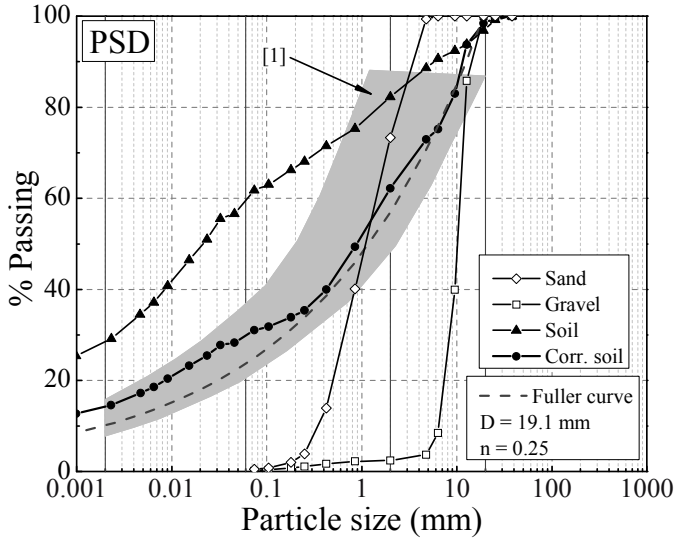

Figure 2: PSD of the selected soil before and after correction.

The excessive clay content of the soil may result in excessive drying shrinkage, whereby it is possible to conclude that this soil is not suitable for this type of construction in its natural state. Furthermore, Table 1 presents the consistency limits and compaction properties of the soil, from where it is highlighted its relatively low maximum dry density (ρ_{dmax}) for URE. In fact, the use of this soil without any PSD correction may result in URE with excessively low strength. Thus, it was decided to proceed with the PSD correction of the soil to manufacture the URE specimens.

LL (%)	PL (%)	PI (%)	ρ_{dmax} (g/cm^3)	OWC (%)	G_s (-)
30	18	12	1.83	13.4	2.68

Table 1: Consistency limits and compaction properties of the soil.

The PSD correction was carried out by means of the addition of river sand and gravel obtained from crushed granite. The PSD curve of the soil after PSD correction (corr. soil) is presented in Figure 2. The correction consisted in adjusting the curve of the mixture of soil, sand and gravel to the Fuller curve of Equation (1), recommended by Houben and Guillaud [1], in order to optimize the density of the URE, and thus its mechanical performance.

$$P = \left(\frac{d}{D} \right)^{0.25} \quad (1)$$

where P is the percentage finer than the size being considered, d is the size being considered and D is the maximum size of the particles. The resulting corrected soil was composed by 50% of soil, 28% of river sand and 22% of gravel (in weight). The properties of the corrected soil are given in Table 2

LL (%)	PL (%)	PI (%)	ρ_{dmax} (g/cm^3)	OWC (%)	G_s (-)
23	16	7	2.10	10.1	2.68

Table 2: Consistency limits and compaction properties of the corrected soil.

2.3 Axial compression tests on URE

The mechanical performance of the rammed earth manufactured with the corrected soil was assessed by performing compression tests on six cylindrical specimens compacted with maximum dry density and OWC. The specimens were compacted with three layers in a metallic mould with dimensions of 100 mm diameter and 200 mm height. The specimens were compacted with an electric rammer and demoulded immediately after. The tests were carried out after the specimens had achieved their equilibrium water content at 20ºC temperature and 57.5% relative humidity (drying period between 27 and 35 days). The axial vertical deformations at the middle third of each specimen were measured by means of three LVDTs radially-disposed. The tests were carried out under displacement control at a rate of 3 μm/s. The top and bottom of the specimens were capped by a layer of gypsum.
The stress-strain curves of the specimens and the respective envelope are given in Figure 3, where the non-linear behaviour of the URE in compression is evidenced. On average, the compressive strength f_c, Young modulus E_0 and equilibrium water content W_{eq} were 1.26 N/mm^2, 1034 N/mm^2 and 1.04%, respectively.

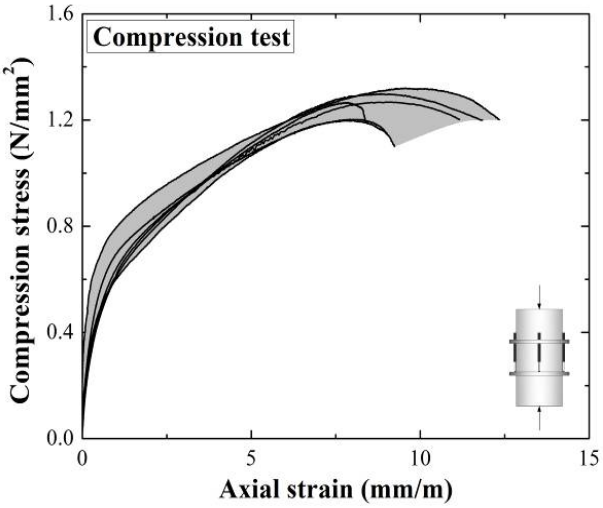

Figure 3: Compression stress-strain curves of the URE cylindrical specimens.

2.4 Diagonal compression tests on URE

A total of eleven URE wallets were tested under diagonal compression. Each specimen was compacted in nine layers of about 61 mm thickness, within a high density plywood mould and resorting to an electric rammer (see Figure 4).

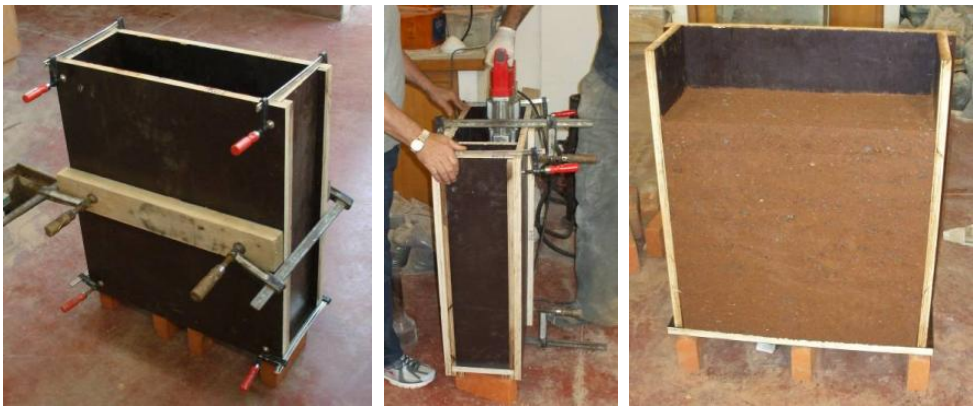

Figure 4: Manufacturing of the URE wallets.

The average dimensions of the wallets were of about 550x550x200 mm^3. The water content of the corrected soil was defined by means of the drop test, see [1]. The water content for compaction was controlled as much as possible, since it was not possible to dry large quantities of material required for manufacturing each wallet in short-time. The water of each material composing the corrected soil was considered for defining the correction weights. The wallets were demoulded immediately after compaction and tested after drying for 12 weeks under a room temperature of about 22±2 ºC. The tests were carried out according to ASTM E519 [16]. The load was applied under monotonic displacement control at a rate of 2 μm/s. The vertical and horizontal displacements were measured in both faces of the wallet, resorting to LVDTs attached to the middle third of each diagonal (see Figure 5).

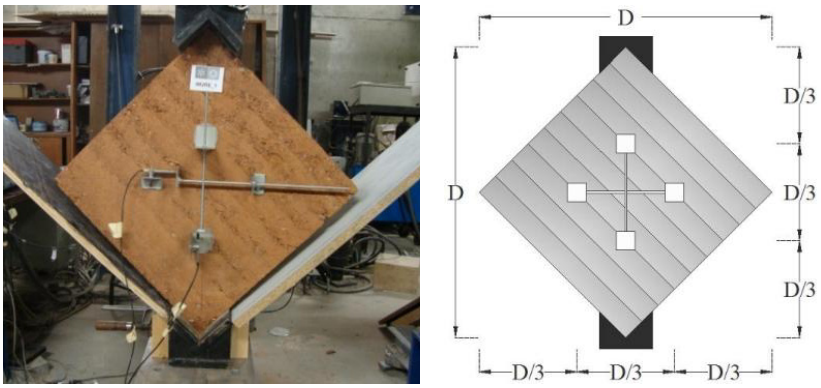

Figure 5: Test setup of the diagonal compression tests.

With respect to the results of the tests, the average values for the shear strength f_s and shear modulus G_0 were 0.15 N/mm^2 and 0.65 N/mm^2, respectively. The shear stress-strain curves of the wallets are presented in Figure 6. In general, these curves are characterized by an early peak shear stress (followed by a huge stiffness loss). This early peak shear stress is thought to be related to cohesion (i.e. to the binding capacity) promoted by the clay fraction. In fact, the shear behaviour of the wallets up to this peak stress is thought to result from the contribution of the clay fraction to cohesion, and friction and interlocking capacity of the gravel-size (or larger) aggregates. After this point, the contribution of the cohesion is thought to be lost and the shear behaviour of the wallets relies only on friction and interlocking.

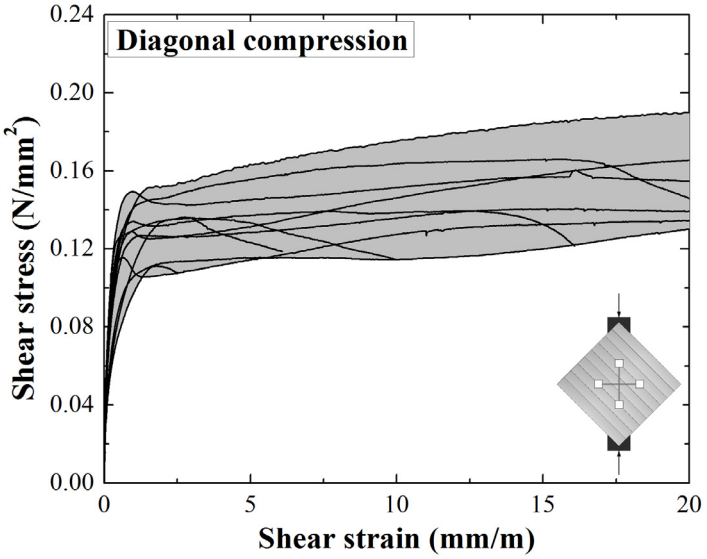

Figure 6: Shear stress-strain curves of the URE wallets tested under diagonal compression.

However, some wallets present a hardening behaviour after the pronounced stiffness loss, which can be explained by a superior interlocking occurring in these wallets. Another important contribution of the friction and interlocking to the shear behaviour of the wallets is that all wallets present large shear deformation capacity, and thus good displacement capacity. This is an important feature for rammed earth in the case of a seismic event, which is expected to contribute to energy dissipation.
In general, the failure of the wallets is characterized by the formation of a main crack or set of cracks with diagonal orientation and crossing the entire specimen, as illustrated in Figure 7 for one of the specimens. The formation of these cracks was observed visually to start at the middle of specimens before the peak load, and then progressing towards the supports. Cracking at the interfaces between layers was also observed, where the diagonal systems of cracks tended to follow partially this interface. Cracks also appeared at the borders of the wallets in the interfaces between layers, developing towards the middle. This observation shows that these interfaces can behave as weakness surfaces, where delamination failure might occur when the material is sheared or tensioned due to a seismic event, for instance.

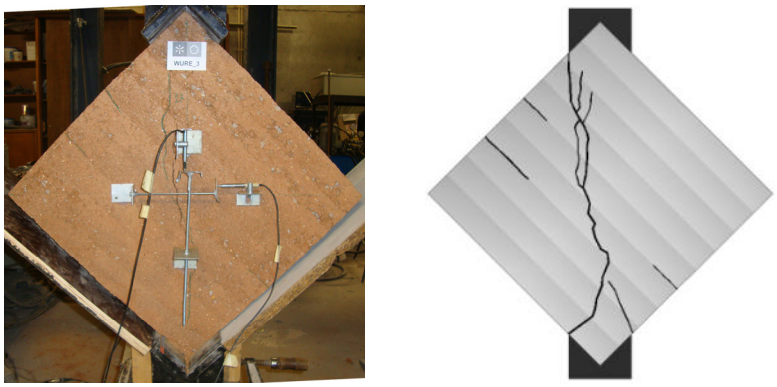

Figure 7: Crack pattern at failure of one of the URE wallets (WURE_3).

3 Numerical modelling

3.1 Geometry, boundary conditions and loading

The numerical simulation of the diagonal compression tests was carried out resorting to the FEM software DIANA 9.4 [17]. The average dimensions of the specimens tested were taken as the dimensions of the numerical model and a plane stress state was assumed. Eight-noded quadrilateral elements (CQ16M) were used to simulate the rammed earth material in both macro- and micro-modelling approaches. In the micro-modelling approach, interfaces between layers were simulated resorting to six-noded zero thickness interface elements (CL12I). The macro-model was constituted by 484 eight-noded elements, while the micro-model was constituted by 594 eight-noded elements and 176 interface elements. The boundary conditions were defined by considering a width of the supports of about 100 mm. The supports were considered as providing full confinement and the load was applied by imposing vertical displacements on the constrained nodes at the top of the model. The self-weight of the material was not considered in the analyses, since its contribution for the stress state was expected to be marginal.

3.2 Constitutive laws

The total strain rotating crack model (TSRCM) was selected to simulate the behaviour of the rammed earth material [17]. The TSRCM corresponds to a model of distributed and rotating cracks based on total strains, where the crack direction rotates with the principal strain axes [18-20]. The TSRCM implemented in DIANA software [17] integrates several possible non-linear stress-strain relationships according to the type of stress involved, namely compression and tension. A multi-linear relationship based on the average curve of the axial compression tests was adopted (see Figure 8a), which allows a more adaptable simulation of the compressive behaviour. The second point of the multi-linear relationship was defined for $0.3f_c$ by taking into account the experimental Young's modulus. The relationship in tension was assumed to be exponential, as depicted in Figure 8b.

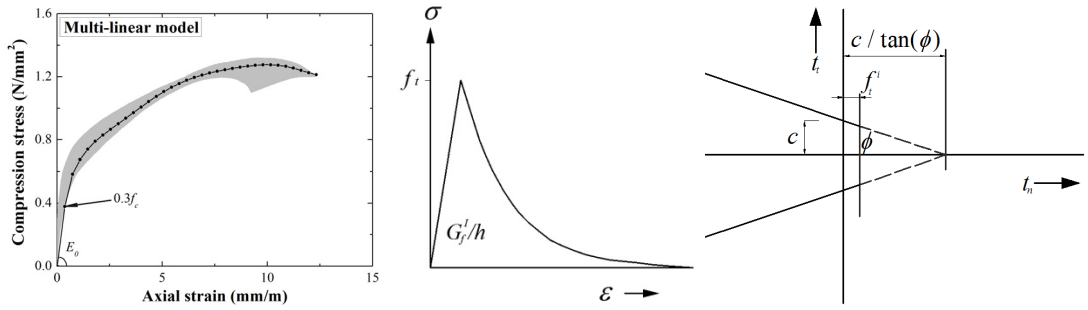

Figure 8: Material models adopted in the numerical modelling: (a) stress-strain relationship in compression; (b) stress-strain relationship in tension; (c) Coulomb friction model used in the interfaces.

The crack bandwidth (h) of the elements was assumed to be dependent of the area of the element (A), according to Equation (2). This assumption allows making the results of the numerical analysis independent from the size of the finite element mesh.

$$h = \sqrt{A} \tag{2}$$

Table 3 presents the initial values assumed for the parameters required by the TSRCM. The average value of the Young's modulus (E_0) obtained from the axial compression tests was used were used in the models. The initial value of the Poisson's ratio (υ) was assumed as 0.27, which corresponds to a value found in the bibliography [21]. The initial values of the remaining parameters were assumed with basis on recommended values for masonry. The tensile strength (f_t) was estimated as $0.1f_c$ and the mode-I tensile fracture energy (G_f^I) as $0.029f_t$.

Material	E_0 (N/mm^2)	υ (-)	f_t (N/mm^2)	G_f^I (N/mm)
Rammed earth	1034	0.27	126	0.0037

Table 3: Initial values of the parameters assumed for the TSRCM of the rammed earth layers.

The Coulomb friction model (Figure 8c) implemented in DIANA software [17] was adopted in the case of interface elements. The parameters required by this model were neither determined experimentally nor available in the literature for the case of URE. This means that these parameters had to be carefully estimated and the initial values are presented in Table 4. The initial values of the interface normal stiffness (k_n) and of the shear stiffness (k_t) were assumed to be very high, to avoid concentrating the elastic deformations in the interface elements. Therefore, k_n was assumed as $100E_0$ and k_s was estimated resorting to Equation (3). These values were shown to be adequate in numerical models simulating the compression behaviour of URE [15]. The cohesion (c) was estimated as a function of the tensile strength, namely as $1.5f_t$. The friction angle (ϕ) was assumed to be 37º and the dilatancy angle

(ψ) as zero. The tensile strength of the interfaces (f_t^i) was defined as $2/3f_t$, while taking into account that the maximum value mathematically allowed by the model is $c/\tan(\phi)$. Finally, the tensile behaviour of the interfaces was assumed as brittle.

Material	k_n (N/mm^2)	k_t (N/mm^2)	c (N/mm^2)	tan(ϕ) (-)	tan(ψ) (-)	f_t^i (N/mm^2)
Interfaces	1.03x10^5	0.41x10^5	189	0.754	0	84

Table 4: Initial values of the parameters assumed for the Coulomb friction model of the interfaces between layers.

$$k_s = \frac{k_n}{2(1+\nu)} \tag{3}$$

3.3 Calibration of the models and results

Figure 9a presents the shear stress-shear strain curves of the macro- and micro-model using the initial values. Both models present similar curves and a behaviour much more brittle than that of the experimental curves. Moreover, the shear strength seems to be overestimated. This means that the calibration of the models requires adjusting both G_f^I and f_t, as well as their relationship.

Figure 9b depicts the curves of the calibrated models, which resulted from an increase of G_f^I of about 20 times and a decrease of f_t in about 2 times. Rammed earth features a broad PSD, which is believed to have a great contribution to the interlocking at the crack surface, by promoting its roughness. This enhances the fracture energy of rammed earth relative to historical masonry, where cracking occurs mostly at less rough surfaces, namely at the interfaces between mortar and masonry units. Furthermore, the calibration of the micro-model also required adjusting f_t^i, which was assumed to be equal to the calibrated value of f_t.

The shear stress-shear strain curve of the macro-model is characterized by a sudden stiffness change close to peak load, occurred for a relatively low strain, followed by a short hardening behaviour until the maximum shear stress is achieved. This curve fits within the experimental envelope, where the maximum shear stress (0.16 N/mm^2) overestimates the average shear strength in about 7%. The development of the shear stress-shear strain curve of the micro-model is similar to that of the micro-model, but the shear hardening is not so significant. Furthermore, the maximum shear stress obtained from the micro-model (0.14 N/mm^2) underestimates the average shear strength in about 6%. In both cases, the difference between experimental tests and numerical models seems not to be very significant.
The failure mode of both models was also analysed. Figure 10 presents the principal tensile strains obtained for an axial displacement of about 1.8 mm. In the case of the macro-model, the damage is shown to concentrate at the middle of the model and to cross it from one support to the other. This corresponds to the formation of the diagonal system of cracks that characterized the failure mode in the experimental tests. The same is observed for the micro-model, but in addition, it is possible to observe the failure by delamination at some interfaces. A slight deviation of the orientation of the damage seems also to be a consequence of this failure mode.

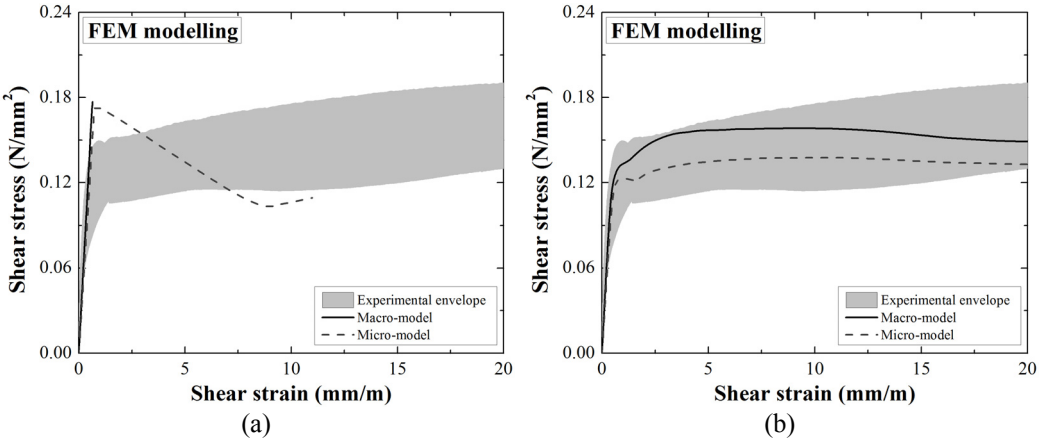

Figure 9: Behaviour of the macro- and micro-model: (a) using the initial parameters; (b) after calibration.

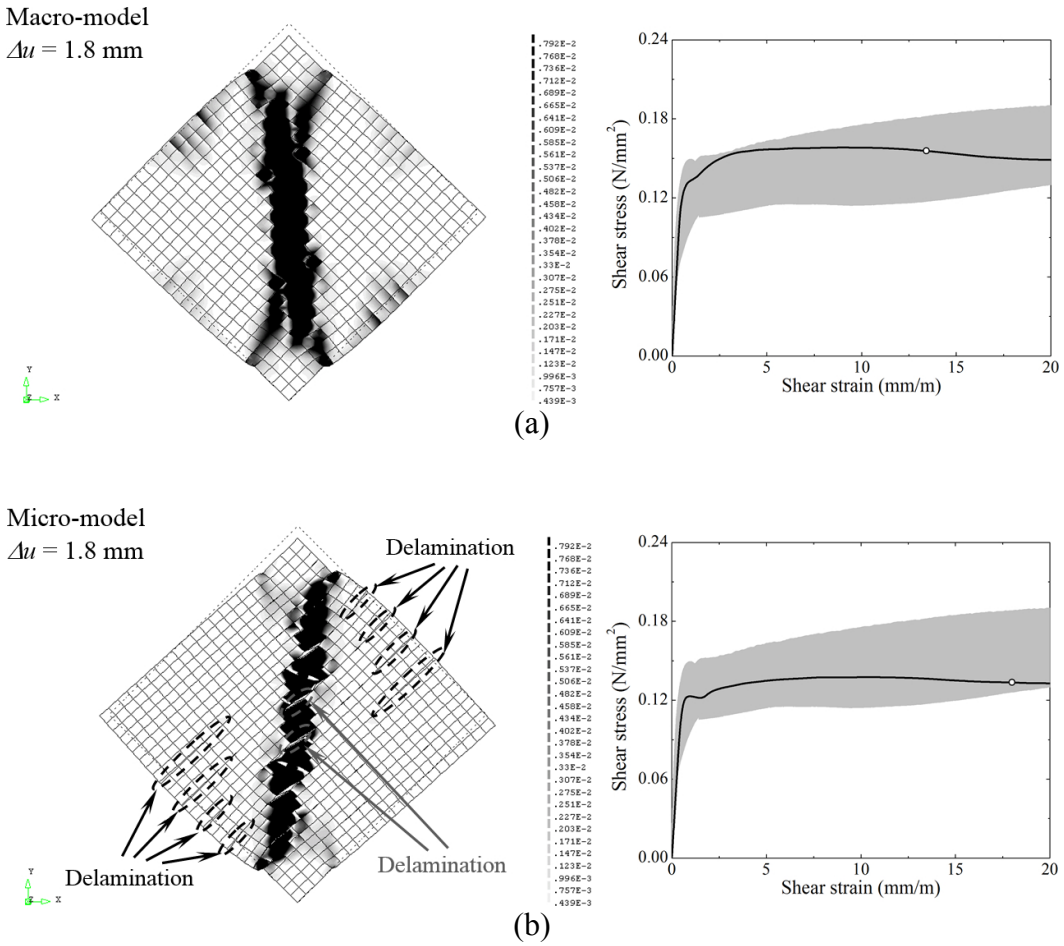

Figure 10: Principal tensile strains for an axial displacement of 1.8 mm: (a) macro-model; (b) micro-model.

4 Conclusions

The shear behaviour of URE was investigated both by means of experimental tests and finite element numerical modelling. The experimental program performed allowed the mechanical characterization of URE manufactured with soil from Alentejo (Portugal), and consisted mainly in the testing of URE wallets under diagonal compression. The compression behaviour of the URE was also characterized and allowed verifying its great non-linear behaviour. The diagonal compression tests allowed verifying a large shear deformation capacity, which is thought to result from friction and interlocking of the coarse aggregates in the URE material.

Then, the non-linear shear behaviour of URE was modelled by simulating the diagonal compression tests and by taking into account both the macro- and micro-modelling approaches. The TSRCM was used to simulate the behaviour of the rammed earth material, while the Mohr-Coulomb failure criterion was used to model the interfaces between layers.

The results from the macro- and micro-models demonstrated to be in good agreement with the experimental envelope of the shear stress-shear strain curves and with the experimental damage pattern. The micro-model allowed capturing the failure by delamination of the interfaces between layers, like observed in the experimental tests. This revealed to be the main advantage of this approach, yet the macro-model seemed to provide an equivalent numerical simulation of the shear behaviour.

Acknowledgments

The authors would like to thank gratefully the funding provided by the Portuguese Science and Technology Foundation through project FCOMP-01-0124-FEDER-028864 (FCT-PTDC/ECM-EST/2396/2012). Furthermore, the authors wish to express their gratitude to Júlio Machado for his valuable help in the experimental program.

References

[1] H. Houben, H. Guillaud, “Earth construction: a comprehensive guide”, CRATerre - EAG, Intermediate Technology Publication, London, 2008.

[2] E. Sebastián, G. Cultrone, “Technology of rammed-earth constructions (“Tapia”) in Andalusia (Spain): their restoration and conservation”, M. Bostenaru-Dan, R. Pøikryl, A. Török eds, Materials, technologies and practice in historic heritage structures, 11-28, 2010.

[3] M. Correia, "Military rammed earth Islamic fortresses", Pedra & Cal, 24, 16, 2004 (in Portuguese)

[4] G. Minke, “Earth construction handbook”, WIT press, Boston, 2003.

[5] P.A. Jaquin, “Analysis of Historic Rammed Earth Construction”, PhD Thesis, Durham University, Durham, 2008.

[6] M. Correia, “Rammed Earth in Alentejo” Argumentum, Lisbon, 2007.
[7] J. Warren, “Conservation of Earth Structure”, Butterworth Heinemann, Bath, 1999.
[8] E.L. Tolles, F.A. Webster, A. Crosby, E.E. Kimbro, “Survey of Damage to Historic Adobe Buildings after the January 1994 Northridge Earthquake”, The Getty Conservation Institute, 1996.
[9] D.V. Oliveira, R.A. Silva, P.B. Lourenço, L. Schueremans, “Rammed earth construction and the earthquakes”, Congresso Nacional de Sismologia e Engenharia. SÍSMICA 2010, Aveiro, Portugal, October 20-23, 2010. (in Portuguese)
[10] P.A. Jaquin, C.E. Augarde, C.M. Gerrard, “Historic rammed earth structures in Spain: construction techniques and a preliminary classification”, International symposium on earthen structures, Bangalore, India, August, 2007.
[11] P.A. Jaquin, C.E. Augarde, C.M. Gerrard, “Analysis of Tapial structures for modern use and conservation”, 4th international conference on structural analysis of historical constructions, November 10-13, Padova, Italy, 1315-1321, 2004.
[12] P.A. Jaquin, C.E. Augarde, C.M. Gerrard, “Analysis of historical rammed earth construction”, 9th Young Geotechnical Engineers Symposium, Belfast, UK, September 4-6, 2006.
[13] I. Gomes, M. Lopes, J. Brito, “Seismic resistance of earth construction in Portugal”, Engineering and Structures, 33, 932-941, 2012.
[14] Q.B. Bui, J.C. Morel, “Assessing the anisotropy of rammed earth”, Constructions and Building Materials, 23, 3005-3011, 2009.
[15] R.A. Silva, “Repair of earth constructions by means of grout injection”, PhD thesis, University of Minho / KU Leuven, Guimarães, Portugal, 2013.
[16] ASTM E519-02: Standard Test Method for Diagonal Tension (Shear) in Masonry Assemblages. American Society for Testing and Materials, West Conshohocken, PA, 2002.
[17] TNO, “Displacement method analyser (DIANA) User's Manual”, Release 9.4, Netherlands, 2009.
[18] J. Figueiras, “Ultimate load analysis of anisotropic and reinforced concrete plates and shells”, PhD Thesis, University of Wales, UK, 1983.
[19] F. Damjamic, D. Owen, “Practical considerations for modeling of post-cracking concrete behavior for finite element analysis of reinforced concrete structures”, International conference on computer aided analysis and design of concrete structures, 693-706, 1984.
[20] R. Póvoas, “Non-linear models of analysis and design”, PhD thesis, University of Porto, Portugal, 1991. (in Portuguese)
[21] L. Miccoli, U. Müller, P. Fontana, “Mechanical behaviour of earthen materials: A comparison between earth block masonry, rammed earth and cob”, Construction and Building Materials, 60, 327-339, 2014.